Observation of large-scale traveling ionospheric disturbances of auroral origin by global GPS networks

Edward L. Afraimovich, Eugene A. Kosogorov, Ludmila A. Leonovich, Kirill S. Palamartchouk,
Natalia P. Perevalova, and Olga M. Pirog

Institute of Solar-Terrestrial Physics SD RAS, P. O. Box 4026, Irkutsk 664033, Russia

The intention in this paper is to investigate the form and dynamics of large-scale traveling ionospheric disturbances (LS TIDs) of auroral origin. We have devised a technique for determining LS TID parameters using GPS arrays whose elements can be selected from a large set of GPS stations forming part of the international GPS network. The method was used to determine LS TID parameters during a strong magnetic storm of September 25, 1998. The North-American sector where many GPS stations are available, and also the time interval 00:00–06:00 UT characterized by a maximum value of the derivative Dst were used in the analysis. The study revealed that this period of time was concurrent with the formation of the main ionospheric trough (MIT) with a conspicuous southward wall in the range of geographic latitudes 50–60° and the front width of no less than 7500 km. The auroral disturbance-induced large-scale solitary wave with a duration of about 1 hour and the front width of at least 3700 km propagated in the equatorward direction to a distance of no less than 2000–3000 km with the mean velocity of about 300 m/s. The wave front behaved as if it 'curled' to the west in longitude where the local time was around noon. Going toward the local nighttime, the propagation direction progressively approximated an equatorward direction.

1. Introduction

Many publications, among them a number of thorough reviews (Hunsucker, 1982; Hocke and Schlegel, 1996) have been devoted to the study of large-scale traveling ionospheric disturbances (LS TIDs) with typical periods of 1–2 hours and 1000–2000 km wavelengths. It is generally accepted that LS TIDs represent the manifestation of acoustic-gravity waves (AGW) whose generating regions lie in the auroral zones of the northern or southern hemisphere. Therefore, research on LS TIDs can provide important information about the processes occurring in these zones under quiet and disturbed conditions.

However, the basic properties and parameters of LS TIDs are as yet imperfectly understood. Are they a periodic process or a solitary wave propagating to large distances from the source of generation? What is the form and the width of the wave front of LS TIDs? Solving the above-mentioned outstanding questions requires appropriate spatial-temporal resolution which cannot be provided by existing highly sparse ionosonde networks, much less by incoherent scatter radars and MST-radars.

An opening shot in a new chapter of remote probing of the ionosphere is the development of a global navigation system GPS and the creation (on its basis) of a far-flung worldwide GPS network numbering about 700 GPS receivers as of April 2000.

We suggest the method of using the GPS network to determine LS TID characteristics. The method is based on calculating spatial and temporal gradients of electron density from TEC measurements at three spaced GPS stations (GPS array). It was implemented for determining LS TID parameters during a strong magnetic storm of September 25, 1998.

2. Methods of Determining the Form and Dynamics of TIDs from TEC Measurements Acquired by GPS Arrays

The method of determining the form and propagation velocity and direction of TIDs which we suggest in this paper is based on Mercier's (1986) statistical method of analyzing the spatial properties of TEC perturbations, recorded by a radio astronomical interferometer with a short baseline ('short' in relation to the TID wavelength).

Thus Mercier's (1986) method gives no way of calculating the velocity modulus, and all that can be achieved is to determine the direction of a normal to the traveling leading edge of TEC. In this case this angle is determined only to within 180°.

In an attempt to achieve a more accurate determination of TID parameters by exploiting the new possibilities made available by the GPS network, Afraimovich *et al.* (1998) have developed the Statistical Angle-of-Arrival and Doppler Method (SADM-GPS). The method, in essence, implies that not only the spatial $I'_x(t)$, $I'_y(t)$ (as in Mercier, 1986) but also time $I'_t(t)$ derivatives of TEC can be determined from measurements of the total electron content $I_A(t)$, $I_B(t)$, and $I_C(t)$ at three spaced GPS stations (GPS array). This furnishes a means of uniquely inferring the orientation $\alpha(t)$ of the TID wave vector K in the range 0–360°, as well as

determining the velocity modulus $v(t)$.

In a first approximation LS TIDs, which propagate in the equatorward direction from the auroral zone, may be represented as a plane solitary traveling wave (Hunsucker, 1982):

$$I(t, x, y) = A \sin(\Omega t - K_x x - K_y y + \varphi_0) \qquad (1)$$

where $I(t, x, y)$ is the TEC; A is the amplitude; K_x, K_y, Ω are the x- and y-projections of the wave vector $\boldsymbol{K}$, and the angular disturbance frequency, respectively; φ_0 is the initial disturbance phase.

Using the SADM-GPS algorithm it is possible to determine at every instant the propagation velocity modulus $v(t)$ and the azimuth $\alpha(t)$ of the LS TID motions by formulas:

$$\alpha(t) = \mathrm{atan}(u_y(t)/u_x(t)),$$
$$v(t) = (v_x^2(t) + v_y^2(t))^{1/2},$$
$$u_x(t) = I_t'(t)/I_x'(t) = u(t)/\cos\alpha(t),$$
$$u_y(t) = I_t'(t)/I_y'(t) = u(t)/\sin\alpha(t), \qquad (2)$$
$$u(t) = |u_x(t)u_y(t)|/(u_x^2(t) + u_y^2(t))^{-1/2},$$
$$v_x(t) = u(t)\sin\alpha(t) + w_x(t),$$
$$v_y(t) = u(t)\cos\alpha(t) + w_y(t),$$

where u_x and u_y are the propagation velocities of the phase front along the axes x and y in a frame of reference related to the GPS array; w_x and w_y are the x and y projections of the velocity w of the subionospheric point (for taking into account the motion of the satellite). Axes x and y are directed eastward and northward, respectively. The azimuth $\alpha(t)$ is measured from y-axis in the clockwise way.

The series $I_A(t)$, $I_B(t)$, and $I_C(t)$ are calculated from increment data on the phase path of the GPS transionospheric signal at two GPS frequencies L_1 and L_2. The method of reconstructing TEC variations from measurements of phase path increments is described in detail and validated in a whole series of publications (for example, Afraimovich *et al.*, 1998).

For determining LS TID propagation characteristics, use is made of continuous series of measurements of a length of two–three hours at least. Variations of the regular ionosphere, and also trends introduced by the motion of the satellite are eliminated using the procedure of filtering the TEC perturbation by removing the trend with third-to-fifth order polynomials. After the trend has been removed, there remain oscillations with a period of about 1 hour, which, with the velocities 200–300 m/s obtained (see below), corresponds to about 1000 km wavelength of the ionospheric irregularities.

The resulting series $I_x'(t)$, $I_y'(t)$, and $I_t'(t)$ are used to calculate instantaneous values of the velocity modulus $v(t)$ and the azimuth $\alpha(t)$ of TID propagation. Concurrent with this procedure, a correction for the motion of the satellite is introduced into calculations using current information about the satellite's angular coordinates (formulas (2)).

Next, the series $v(t)$ and $\alpha(t)$ are put to a statistical treatment. This involves constructing distributions of the velocity $P(v)$ and direction $P(\alpha)$ which are analyzed to test the hypothesis of the existence of the preferred propagation direction. If such a direction does exist, then the corresponding

distributions are used to calculate the mean value $\langle v \rangle$ and the r.m.s. σv of the velocity modulus, as well as the mean value $\langle \alpha \rangle$ and the r.m.s. $\sigma \alpha$ of the azimuth of TID propagation.

Thus through the use of the transformations (2) we obtain the following parameters characterizing the TID dynamics (see Table 2): T_0 is the start of measurements; dT is the time interval of measurements; A is the amplitude of the filtered TEC which is determined as the r.m.s. of the series $I_B(t)$; $\langle \alpha \rangle$ and $\sigma \alpha$, respectively, are the mean value and the r.m.s. of the LS TID propagation direction; and $\langle v \rangle$ and σv, respectively, are the mean value and the r.m.s. of the velocity modulus.

Also for comparison purposes, we resorted to a possibility of estimating the LS TID propagation velocity from the time lag of such TEC variations at meridionally spaced points. For the central point of each array, we decided to choose a longitudinally near-lying but higher-latitude calibrating station, at which TEC variations had the character similar to those at the central point but occurring somewhat earlier. This time lag was used to determine the LS TID propagation velocity v_r along the calibrating station—GPS array central point line.

3. Characteristics of the Geomagnetic Situation on September 25, 1998, and the Experimental Geometry

Our developed method was implemented for determining LS TID parameters during a strong geomagnetic disturbance on September 25, 1998. On that day, Dst variations showed a large storm with a maximum amplitude of 233 nT. Kp in the storm maximum were as high as 8, and the sum of Kp for 24 hours was 48 on September 25.

Within the context of this study, we will focus our attention on the determination of the LS TID properties which occurred in the auroral zone in the most interesting time interval 00:00–04:00 UT characterized by the largest value of the Dst derivative. The values of Dst variation and Kp-index for September 24 and 25 are shown in Fig. 1, panels b and c.

The initial TEC series $I(t)$ for the same satellite, PRN19, for the time interval 00:00–04:00 UT 25 September 1998, which were calculated for the set of auroral stations (see left part of Table 1) and were brought to the 'vertical' value by the familiar technique (Calais and Minster, 1995) are presented in Fig. 1 on panel a.

In this paper we limit ourselves only to TEC variations obtained from phase delay GPS measurements. For definiteness sake, we bring the TEC variations into the region of positive values with the minimum value equal to 0.

Almost all of auroral stations exhibit a gradual growth of TEC until about 02:00 UT, as well as an abrupt decrease and a pronounced inhomogeneous structure of TEC subsequent to the intersection of this time mark. One plausible interpretation of these data implies that the beams to the satellite in the given time interval intersected the southward wall of the main ionospheric trough (MIT).

An important point within the framework of this paper is that throughout the set of auroral stations the depth of the MIT inferred from the value of relative variation (abrupt decrease) of TEC reached a very large value (from 15 to 25 TECU, TECU = 10^{16} m^{-2}). According to the concepts summarized in a review by Hunsucker (1982), such an extended region of
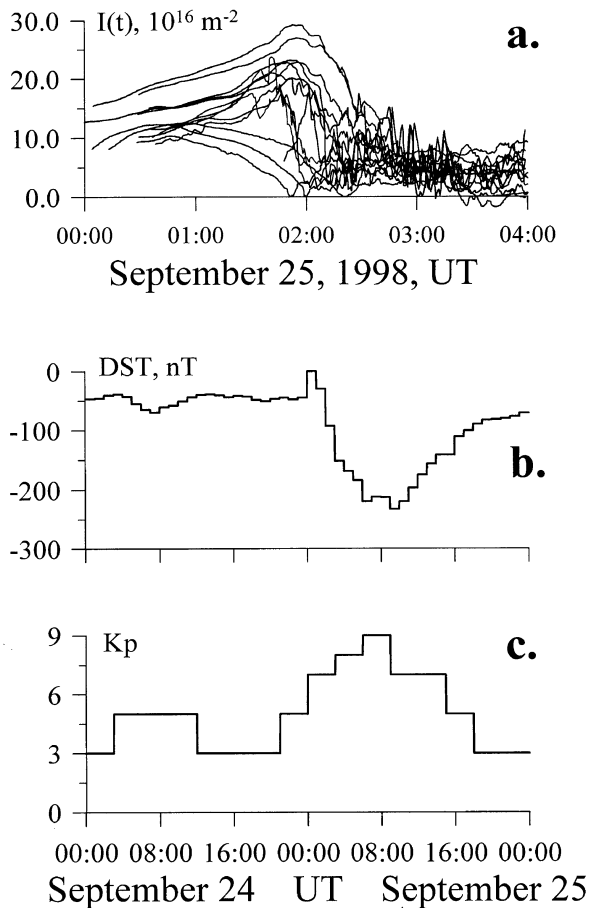
Fig. 1. TEC series $I(t)$ (a) as obtained during the magnetic storm of September 25, 1998 by the set of auroral stations (see left part of Table 1). *Dst* variations of the geomagnetic field (b) and Kp-index (c) during a strong geomagnetic storm of September 24–25, 1998.

the auroral ionosphere that was disturbed so rapidly from an equilibrium condition for a short time interval, must become a source of strong LS TIDs propagating toward the equator.

For a reliable determination of LS TID characteristics, it was necessary to detect them at distances larger than the expected wavelength (over 1000 km) and along the entire expected wave front (up to several thousand kilometers). It is primarily these considerations which dictated the selection of corresponding GPS arrays. Furthermore, it was important to choose areas with a sufficiently dense network of stations such as to ensure appropriate distances between sites of the GPS arrays.

In addition to assess the presence of TIDs in other geographic regions we succeeded in select a further two suitable arrays: one in England (with central site BRUS), and the other in the southern hemisphere (with central site ORRO, Australia).

Geographic coordinates of all GPS-sites used in this paper are presented in Table 1.

4. The Form and Dynamics of LS TIDs as Deduced from Interferometer Data

The data obtained were processed in full conformity with the procedures and formulas described in Section 2. The corresponding parameters are collected in Table 2.

Figure 2 presents the time dependencies of the $I(t)$ series for the central site of each GPS array. Names of the central sites and GPS satellite numbers, for which the data were obtained, are given in bold print. For comparison, the panels present also the plots of $I(t)$ for calibrating sites from the set of auroral stations whose names are given in light print.

For qualitative comparison with the data from the North-American sector, Fig. 2 also presents results for the GPS arrays located in England and in the eastern part of the southern hemisphere.

The outliers of the direction and velocity in Fig. 2, panels (e)–(f), (h)–(i), (k)–(l), and (n)–(o), are due to a simplified approach to modeling TIDs when developing SADM-GPS. SADM-GPS assumes that a TID has an ideal plane front described by formula (1), which is equivalent to the neglect of second-order correction when deriving formulas (2). In real situations, however, fronts can be more complicated in shape where nonsimultaneous changes of signs of $I'_x(t)$, $I'_y(t)$, and $I'_t(t)$, which are impossible in the case of a perfectly plane front, can give 'whistlers' as observed in Fig. 2. However, a verification of SADM-GPS, described by Afraimovich *et al.*, (1998), revealed that with a statistical approach to the resulting series of TID directions and velocities, their mean values inferred using SADM-GPS are similar to true ones. Thus the outliers are an artifact; they are actually nonexistent and do not interfere with a further statistical analysis of the data.

LEEP interferometer consists of three stations: LEEP, CVHS, and DYHS. The distances between the central and outlying sites do not exceed 40 km. It is clearly seen in Fig. 2a that a sharp TEC peak $I(t)$ occurred at 04:00 UT (20:00 LT) at the LEEP station at the background of a quiet evening decrease in TEC, which is quite extrinsic to this time of day for magnetically quiet conditions but is highly characteristic for TEC variations as pointed out by many authors for similar disturbed conditions. It should be noted that in Table 2 the quantity A represents the standard deviation of the filtered TEC; therefore, its value is by a factor of 2–3 lower than the oscillation range in Fig. 2.

Such TEC variations (Fig. 2a) were observed approximately two hours earlier at the DRAO station located at the distance of 1659 km along the great-circle arc to the north of the LEEP array. This delay corresponds to the velocity v_r of LS TID propagation along the DRAO-LEEP line, equal to 212 m/s.

Figure 2 presents the time dependencies of the direction $\alpha(t)$—panel b and the phase velocity modulus $v(t)$ of LS TIDS—panel c as determined for the LEEP array using the SADM-GPS method by formulas (2).

The mean value of the velocity modulus $\langle v \rangle$ is 254 m/s, which, with the period of the wave of about 1 hour, corresponds to 1000 km wavelength, typical of LS TIDs. It is close to the value of $v_r = 212$ m/s as determined from the wave delay along the DRAO–LEEP line. The mean value of $\langle \alpha \rangle = 245°$ and this direction differs noticeably from the equatorward direction.

As an assurance of the reliable determination of the main parameters of the form and dynamics of LS TIDs by formulas (2), in the area of South California near the LEEP array we chose other variants of GPS-arrays and processed the

Table 1. GPS site names and locations.

N	SITE	Geogr. lat.	Geogr. long.	N	SITE	Geogr. lat.	Geogr. long.
	Auroral stations				GPS array stations		
1	AIS1	55.1	228.4	1	BRAN	34.2	241.7
2	ALGO	46.0	281.9	2	CSDH	33.9	241.7
3	DRAO	49.3	240.4	3	CVHS	34.1	242.1
4	DUBO	50.3	264.1	4	DYHS	33.9	241.9
5	FAIR	65.0	212.5	5	LEEP	34.1	241.7
6	KEW1	47.2	271.4	6	UCLP	34.1	241.6
7	NANO	49.3	235.9	7	UCS1	34.0	241.7
8	POR2	43.1	289.3	8	LMNO	36.7	262.5
9	PRDS	50.9	245.7	9	HVLK	37.7	260.9
10	SEAT	47.7	237.7	10	VCIO	36.1	260.8
11	SEDR	48.5	237.8	11	HNPT	38.6	283.9
12	WHIT	60.8	224.8	12	USNO	38.9	282.9
13	WILL	52.2	237.8	13	VIMS	37.6	284.3
14	WSLR	50.1	237.1	14	BRUS	50.8	4.4
15	KELY	67.0	309.1	15	DOUR	50.1	4.6
16	MAC1	−54.5	158.9	16	WARE	50.7	5.3
				17	ORRO	−35.6	148.9
				18	STR1	−35.3	149.0
				19	TID1	−35.4	149.0

Table 2. LS TID parameters as derived from GPS measurements.

SITE	T_0, UT	A, TECU	$\langle\alpha\rangle$, °	$\sigma\alpha$, °	$\langle v\rangle$, m/s	σv, m/s	v_r, m/s
LEEP, CVHS, DYHS	2.28	2.634	245	22	254	148	212
USC1, UCLP, LEEP	2.30	2.498	260	28	362	224	
DYHS, BRAN, UCLP	2.31	2.560	249	27	322	204	
CVHS, LEEP, CSDH	2.32	2.595	236	23	351	218	
LMNO, HVLK, VCIO	2.82	0.480	195	24	264	236	238
USNO, HNPT, VIMS	2.41	0.648	177	37	211	138	154
BRUS, DOUR, WARE	3.58	0.335	175	17	286	244	364
ORRO, TID1, STR1	7.72	0.958	331	44	324	158	241

data with the same processing parameters as for the LEEP array. Statistical data presented in Table 2 (lines 2–4) show an agreement of the mean values within their r.m.s., which is testimony to good stability of the acquired data irrespective of the GPS-array configuration.

For the same time interval as for LEEP, Fig. 2 presents the time dependencies of TEC, as well as the directions and phase velocity moduli TIDs as determined by LMNO array.

Corresponding values of statistical characteristics are given in Table 2. One can notice the proximity of all mean values to corresponding parameters for the LEEP array, except that the mean value $\langle\alpha\rangle$ is now closer to the equatorial value (195°) and the wave amplitude is by a factor of 5 smaller than that for LEEP. The mean value of the velocity modulus $\langle v\rangle$, equal to 264 m/s, is also close to the value of $v_r = 238$ m/s determined from the wave delay along the DUBO-LMNO line.
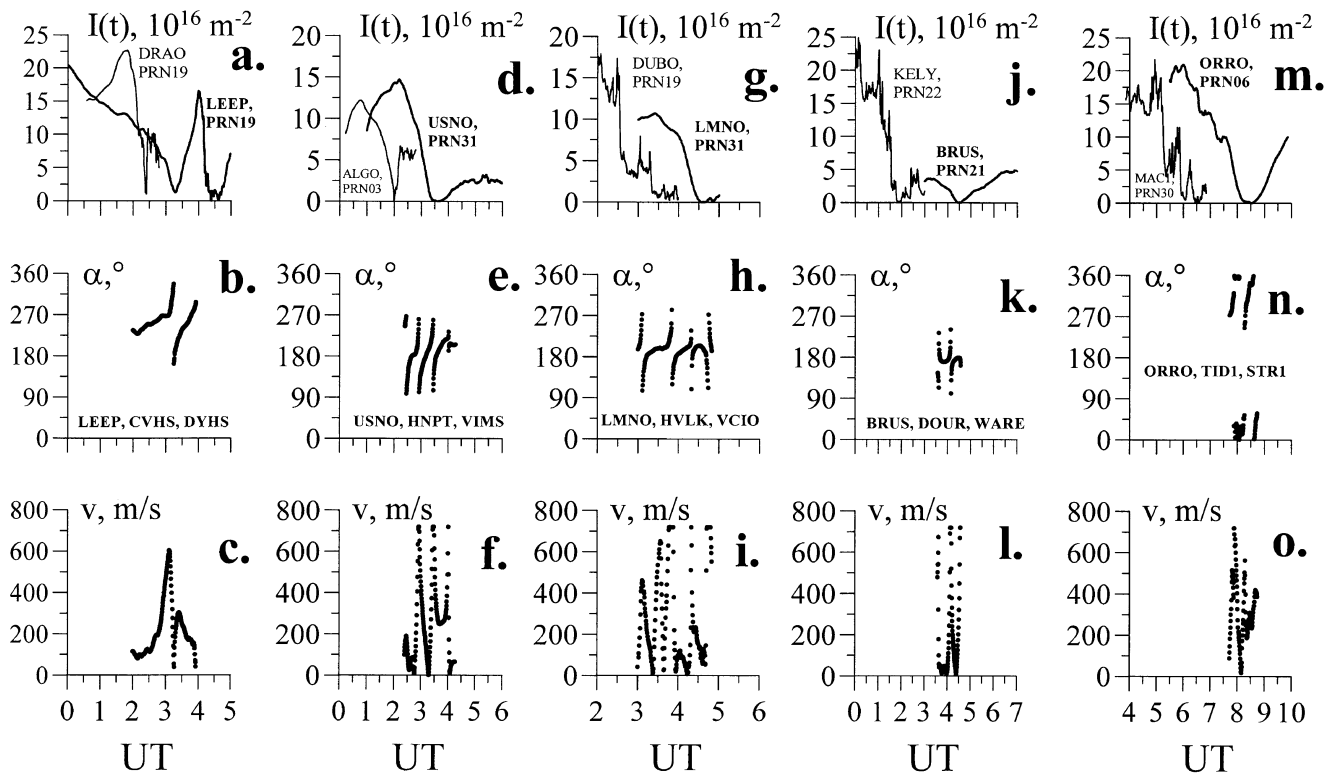
Fig. 2. Time dependencies of the $I(t)$ (a, d, g, j, m), the direction of the wave vector $\alpha(t)$ (b, e, h, k, n), and the phase velocity modulus $v(t)$ of LS TIDs (c, f, i, l, o) as determined by the SADM-GPS method for GPS arrays LEEP (a, b, c), USNO (d, e, f), LMNO (g, h, i), BRUS (j, k, l), ORRO (m, n, o). Thin lines in panels a, d, g, j, and m show the dependencies $I(t)$ for the calibrating site whose names are given in light print.

Similarly, Fig. 2 presents the time dependencies of TEC as well as the directions and phase velocity moduli of LS TIDs, as determined for the USNO array. Corresponding values of statistical characteristics are given in Table 2. Unlike LEEP and LMNO, the direction of LS TID propagation is nearly equatorward, and the mean value of the velocity modulus $\langle v \rangle$ is markedly smaller (211 km/s). Also, the value of v_r determined from the wave delay along the ALGO-USNO line is still smaller (154 m/s).

For the time interval 00:00–07:00 UT, Fig. 2 presents the time dependencies of TEC, as well as the directions and phase velocity moduli of LS TIDs, as determined for the BRUS array in England—see also line the Table 2. The mean values are very close to corresponding parameters for the LMNO array. However, $\langle v \rangle$ equal to 286 m/s is markedly smaller than the value of $v_r = 364$ m/s as determined from the wave delay along the KELY-BRUS line.

Some authors pointed out a similarity or even a synchronism of the generation of LS TIDs in the northern and southern hemisphere during geomagnetic disturbances (Hajkowicz and Hunsucker, 1987). Unfortunately, the possibilities of choosing a suitable array in the southern hemisphere have been hitherto limited because of relatively sparse coverage of the GPS network. For the time interval described here, we were able to locate only one GPS array ORRO, the data from which are presented in Fig. 2 and in Table 2. As expected, the propagation direction $\langle \alpha \rangle$ was equatorward as before; however, a marked (by 30°) westward deviation of the direction must also be pointed out in this case.

5. Discussion and Conclusions

As has been pointed out in Section 1, some researchers have reported markedly differing values of the LS TID propagation velocity—by as many as several thousand m/s, or exceeding the sound velocity at heights of AGW propagation in the atmosphere (see reviews of Hunsucker, 1982; Hocke and Schlegel, 1996).

High velocity values were obtained for the most part at meridionally spaced 'chains' of ionosondes (as far as was allowed by actual possibilities). For example, Hajkowicz and Hunsucker (1987), by investigating the propagation of LS TIDs from variations of F-region effective heights in the northern and southern hemisphere, found that large-scale disturbances of ionization propagate equatorward with the velocity of about 800 m/s and have a constant period of about 135 min in both hemispheres. Similar results were obtained at spaced sites of TEC measurement from geostationary satellite signals and from ionosonde chains in a paper of Yeh *et al.* (1994).

The authors of the cited papers constructed a dependence of the time delay of similar disturbances of the received signal parameters on the latitude of the point of observation. Therefore, the meridional velocity component of the disturbance front rather than the true phase velocity of LS TID propagation was actually estimated. This velocity was equal to the phase velocity, provided that LS TIDs propagated exactly equatorward. With a marked deviation from the southward direction, such a method could give obviously too high estimates of the propagation velocity of LS TIDs. For the LEEP

array, for example, where we observed the largest possible (in relation to the data from the other arrays) deviation from the equatorward direction of LS TID propagation, such an apparent velocity value would be 604 m/s, or more than twice as large as the true value of the phase velocity (254 m/s).

It is worth noting that whenever the spaced beam reception method was used at the EISCAT incoherent scatter station to determine the velocity and direction of LS TIDs (Ma *et al.*, 1998), the resulting estimates of the phase velocity of LS TID propagation did not exceed 400 m/s. Still smaller values of the phase velocity of LS TIDs (averaging about 240 m/s) were measured at the MU radar (Oliver *et al.*, 1997). Similar estimates of the LS TID velocity (from 50 to 280 m/s) were obtained at Super-DARN (Hall *et al.*, 1999). These data are in good agreement with the mean value of the phase velocity which we have obtained by taking into account the data from all arrays listed in Table 2 (300 m/s).

It is somewhat surprising that the apparent propagation velocity v_r tends to decrease when compared with the mean velocity $\langle v \rangle$ obtained by using SADM-GPS. Conceivably this is due to considerable differences of the characteristics of the wave front near the region of its generation (auroral zone) and at mid-latitudes where the GPS interferometers are located.

For all arrays, the cross-section of the wave front along the propagation direction was more likely to correspond to a solitary traveling wave than to a periodic process, which is consistent with the data reported by other authors (Hunsucker, 1982). According to our data, the large-scale solitary wave with a duration of about 1 hour that was produced by an auroral disturbance, propagated in the equatorward direction to a distance of at least 2000–3000 km with the mean velocity of about 300 m/s.

The direction of the wave vector $\mathbf{K}$ varied along the wave front from 245° in the LEEP array longitude and 195° in the LMNO longitude to 177° in the USNO longitude. The wave front behaved as if it 'curled' to the west in longitude where the local time was around noon. Going toward the local nighttime, the propagation direction approached the equatorward propagation.

One way of explaining the westward displacement of the propagation direction of LS TIDs could be based on the well-known difference of the positions of the geographic and geomagnetic poles subject to the condition that the region generating LS TIDs in the auroral zone is symmetric about the geomagnetic pole.

Another way to explain such a structure of disturbance wave front was proposed by Foster (1989). According to his model, 'curling' of the disturbance front is the effect of great stream of plasma, ejected from rotating sun-ward polar cap.

Published data on propagation directions of LS TIDs are very few in number. It is generally believed that they move toward the equator. We are aware only of a few papers where numerical values of the propagation azimuth of LS TIDs are given and its westward displacement by 10–20° on average is determined, which is consistent with the concept of the Coriolis force effect on the AGW propagation in the atmosphere (Balthazor and Moffett, 1999; Hall *et al.*, 1999). Our data may be treated as supporting this hypothesis.

However, more reliable conclusions require expanding considerably the sample statistic of GPS arrays used in the analysis of LS TIDs of auroral origin.

References

Afraimovich, E. L., K. S. Palamartchouk, and N. P. Perevalova, GPS radio interferometry of traveling ionospheric disturbances, *J. Atmos. Solar-Terr. Phys.*, **60**, 1205–1223, 1998.

Balthazor, R. L. and R. J. Moffett, Morphology of large-scale traveling atmospheric disturbances in the polar thermosphere, *J. Geophys. Res.*, **104**(A1), 15–24, 1999.

Calais, E. and J. B. Minster, GPS detection of ionospheric perturbations following the January, 1994 Northridge earthquake, *Geophys. Res. Lett.*, **22**, 1045–1048, 1995.

Foster, J. C., T. Turunen, P. Pollari, H. Kohl, and V. B. Wickwar, Multi-radar mapping of auroral convection, *Adv. Space Res.*, **9**(5), (5)19–(5)27, 1989.

Hajkowicz, L. A. and R. D. Hunsucker, A simultaneous observation of large-scale periodic TIDs in both hemispheres following an onset of auroral disturbances, *Planet. Space Sci.*, **35**(6), 785–791, 1987.

Hall, G. E., J.-F. Cecile, J. W. MacDougall, J. P. St.-Maurice, and D. R. Moorcroft, Finding gravity wave source positions using the Super Dual Auroral Radar Network, *J. Geophys. Res.*, **104**(A1), 67–78, 1999.

Hocke, K. and K. Schlegel, A review of atmospheric gravity waves and traveling ionospheric disturbances: 1982–1995, *Ann. Géophysicæ*, **14**, 917–940, 1996.

Hunsucker, R. D., Atmospheric gravity waves generated in the high-latitude ionosphere. A review, *Rev. Geophys.*, **20**, 293–315, 1982.

Ma, S. Y., K. Schlegel, and J. S. Xu, Case studies of the propagation characteristics of auroral TIDs with EISCAT CP2 data using maximum entropy cross-spectral analysis, *Ann. Géophysicæ*, **16**, 161–167, 1998.

Mercier, C., Observations of atmospheric gravity waves by radiointerferometry, *J. Atmos. Terr. Phys.*, **48**, 605–624, 1986.

Oliver, W. L., Y. Otsuka, M. Sato, T. Takami, and S. Fukao, A climatology of F region gravity waves propagation over the middle and upper atmosphere radar, *J. Geophys. Res.*, **102**, 14449–14512, 1997.

Yeh, K. C., S. Y. Ma, K. H. Lin, and R. O. Conkright, Global ionospheric effects of the October 1989 geomagnetic storm, *J. Geophys. Res.*, **99**(A4), 6201–6218, 1994.

E. L. Afraimovich (e-mail: afra@iszf.irk.ru), E. A. Kosogorov, L. A. Leonovich, K. S. Palamartchouk, N. P. Perevalova, and O. M. Pirog